



SERIES RESONANT DC-DC CONVERTER DESIGN AND MANAGEMENT IN HIGH VOLTAGE WIND TURBINES, DC

¹V.Ravikumar, ²E.Gopi, ³Sale Rajesh, ⁴Rathila Rambabu

^{1,2,3}Assistant Professor, ⁴UG Student, ^{1,2,3,4}Dept. of Electrical and Electronics Engineering, Visvesvaraya College of Engineering and Technology, Mangalpalle, Telangana, India.

ABSTRACT

Technology for power conversion is continually changing to suit the demand for higher power density and efficiency. People have started to reevaluate the possible roles of dc systems in current and future electrical systems as a result of the rising usage of renewable energy sources and energy storage in recent decades. DC voltage distribution has been employed in a number of industries, including data centers, the aerospace sector, and dc micro-grids, for its high efficiency and power density. With its benefits of smooth switching and minimal EMI, resonance DC-DC converters are appealing solutions to these issues. The primary goal of this project is to detect and study the converter's working modes using the pulse removal approach. The innovative technique of operation offers transformer size reduction and soft-switching transition of insulated gate bipolar transistors (IGBTs) and line frequency diodes on the rectifier side by using variable frequency and variable phase displacement in sub-resonant mode. The converter employs a revolutionary mode of operation known as pulse elimination technology, which is distinguished by variable frequency and phase shift modulation. Using MATLAB/SIMULINK simulation results, the suggested control approach may be used to identify the reference switching function command to achieve high power efficiency.

INTRODUCTION

Throughout the past 200 years, people have relied on conventional energy sources including coal, petroleum, and other fossil fuel reserves. One of the most significant forms of energy distribution for a long time has been the distribution of electric power energy. Global industrialization and economic development were the results. The primary energy sources are still used to produce electricity, but this has undesirable side effects such as air pollution and other environmental harm. The twenty-first century is predicted to see an increase in global air temperature of 1.5°C. Also, the rising worry about the depletion of resources like petroleum, coal, and natural gas compels people to look for alternative renewable energy sources. As a result of growing concern about nonrenewable resource overconsumption, the development of renewable energy sources has increased. Today, much of the research work in the fields of power electronics, electric motor drive, and electric power system has gone towards the development of alternative electricity generation technologies. Fuel cells, wind production, photovoltaic (PV), wave energy, and hydro-electric generating have been the most widely used renewable energy sources thus far. After many years of study and development, renewable energy resources have recently undergone a greater percentage rise. Renewable energy sources currently generate 19% of the world's electrical energy. Offshore wind power has emerged as a major energy resource in Europe in recent years. The MVAC collection grid could be replaced with MVDC (Medium Voltage Direct Current) grids to boost efficiency and minimise the bill of materials for the technology, lowering the levelized cost of electricity (LCOE) by up to 3%. MVDC grids are predicted to play a significant part in future energy distribution and collection systems. The fault-tolerant component serves to increase the system's supply, and several fault-tolerant solutions have been proposed in the literature. The majority of these approaches include a large amount of additional hardware (such as series connection of switches/fuses or semiconductors/leg redundancy to isolate the failure, increasing the cost and decreasing the device's performance). In this case, the use of the topology's innate fault-tolerant functionality suggests a fault-tolerant resolution with minimal added hardware and no influence on SRC converter performance. Individually from the device, the semiconductor might fail in two ways: open circuit or brief circuit. An OC failure is caused by bond-wire or ruptures, as well as a gate power failure, according to the motives.



The SC failure, on the other hand, is most likely the result of a dynamic or static latch up, an overvoltage, a second breakdown, or an energy shock. Because the majority of disasters occur in a SC environment, this work focuses on an SRC that is resistant to SC failure. In the proposed reconfiguration scheme, the SRC overall bridge in an SRC half-bridge converter is reconfigured. However, considering the same parameters, the output voltage produced by the Half Bridge-SRC is half of the voltage produced by the Full Bridge-SRC. To achieve an equal output voltage, a novel reconfigurable rectifier-based topology with a voltage-doubler is presented.

DISCONTINUOUS CONDUCTION MODE

The inductor current in the energy transfer never approaches zero during continuous conduction mode. The inductor current goes to zero in the discontinuous conduction mode, which is quite common in DC-to-DC converters. If the peak of the inductor current ripples is smaller than the DC component of the inductor current, the diode current is always positive, and the diode is compelled to turn on when switch S (either a transistor or thyristor) is turned off. If the peak of the inductor current waves exceeds the DC component of the inductor current, the total current goes to zero while the diode is conducting. As a result, the diode will cease to conduct and the inductor current will remain zero until the switch S is gated again due to polarity reversal across the switch. This causes the chopper or DC-to-DC converter to operate in the discontinuous conduction mode. In the discontinuous conduction mode, inductor current is not constant throughout the cycle and hits zero even before the period ends. The inductance of the discontinuous conduction mode is less than the minimum value of the inductance of the continuous conduction mode.

$L_{DCM} < L_{CCM}$.

As a result, this scenario frequently occurs for the light-load condition. In the case of the discontinuous conduction mode, let the value of inductance be, $L_{DCM} = \xi L_{CCM}$, where $0 < \xi < 1$ for the discontinuous conduction. The discontinuous conduction mode is most common in converters with single-quadrant switches, although it can also occur in converters with two-quadrant switches. This article will go over two-level DC buck, boost, and buck-boost converters in further detail. For the inductor voltage, two levels are given here approaching the two-voltage level. The inductor's energy storage is proportional to the square of the current flowing through it. With the same power passing through the converter, the inductor current required is greater in the discontinuous conduction mode than in the continuous conduction mode. This increases the losses in the discontinuous conduction circuit. The ringing occurs because the energy held in the discontinuous conduction has not yet been released to the output. In the discontinuous conduction mode, this may also result in noise. Furthermore, the discontinuous conduction mode requires less inductance than the continuous conduction mode since it allows the inductor current to sink to zero.

As a result, the root-mean-square and peak current values increase. As a result, the size of the transformer required in isolated converters is larger than that required in continuous-conduction converters to accommodate the increased flux linkage and losses. When in continuous conduction mode, the conversion ratio is independent of the load; however, when in discontinuous conduction mode, it becomes dependent on the load. Because the first-order equations become second order, the DC-circuit analysis becomes more complicated. The continuous conduction mode is used in the majority of applications. However, discontinuous conduction mode can be used for specific applications such as low-current and loop-compensation.

SYSTEM MODELING

Offshore wind farms currently employ HVAC collecting networks to carry electricity gathered from wind turbines to onshore, however other methods use HVAC up to a big rectifier and then to the mainland through an HVDC transmission line. According to HVdc wind farms, when connected to an MVDC collecting system, they can run more efficiently. Figure 1(a) is a single line diagram of a dc wind farm. The motivation stems from the fact that the levelized cost of energy might be decreased by up to 3% by boosting efficiency

by 2% and lowering the bill of materials prices by at least 1%. MVDC grids are likely to be the primary choice for energy distribution and collection grids in the near future. The MV dc/dc converter situated in the wind turbines is a desirable but difficult component of such a system. A unidirectional SRC could be a solid candidate option with more benefits than deficits. The proposed topology consists of a low voltage (LV) inverter, a monolithic transformer (with one primary and one secondary winding), and a medium voltage (MV) rectifier constructed with series linked diodes. The topology will be denoted as SRC# and is depicted in Fig. 1. (b).

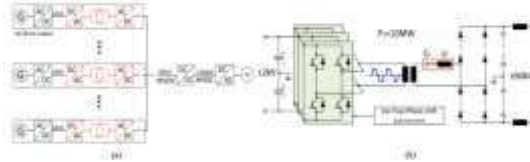


Fig. 1. (a) Single line diagram of dc wind farm; (b) SRC with new method of operation (SRC#).

The dc/dc converter's goals are high availability, efficiency, and power density, which can be achieved with the usage of SRC. Given the HV requirements, a transformer with a high turns ratio should be used. However, leakage inductance in HV transformers can cause large overshoots across the switching semiconductors. The leakage inductance can now be included into the tank and actually aid reduce losses by using a series resonant tank. The topology has mostly been studied in traction applications and solid-state transformers for high-power operation. It is known as half cycle DCM SRC when operated at constant frequency and in sub resonant mode. The converter combines two dc-link voltages with a preset voltage transfer ratio for these applications, but there are no control options [Fig. 2(a)]. In the case of a wind turbine, the dc/dc converter must be capable of managing the LV dc bus voltage while also providing galvanic separation and an HV gain. A candidate solution [Fig. 2(b)] was offered, which utilises an SRC in resonant mode with constant frequency, while a front end boost converter regulates the input dc-link, increasing the number of components, complexity, and losses.

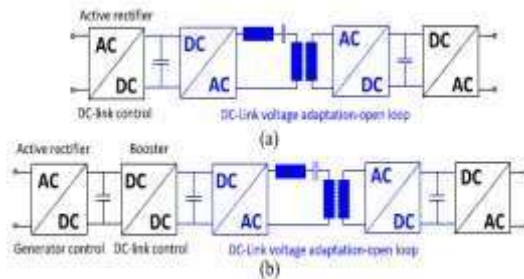


Fig. 2. (a) Turbine converter with SRC operated in subresonant mode at constant frequency in open loop; (b) Concept with dc/dc converter operated at resonant mode and constant frequency in open loop.

Theory of Operation

A study of SRC modes of operation and control is required to completely appreciate the pulse elimination technique. Consider the first SRC design, with the tank on the inverter side, as illustrated in Fig. 3, where the transformer magnetising inductance L_m is originally ignored. When the two complementary switching pairs (S1, S2) and (S3, S4) alternately open and close, a square wave voltage V_g with a set frequency F_{sw} and duty cycle D is delivered to the resonant LC tank while the rectifying bridge is left unregulated, i.e., just diodes are in operation. The tank's resonant frequency F_r , resonant angular frequency ω_r , and characteristic impedance are all defined further. In the tank circuit, V_g produces a resonant current i_{rp} , which is rectified and filtered before being delivered into the output voltage network. The ratio of F_{sw} to F_r determines the amount and form of the output current. This explanation applies to all forms of functioning,

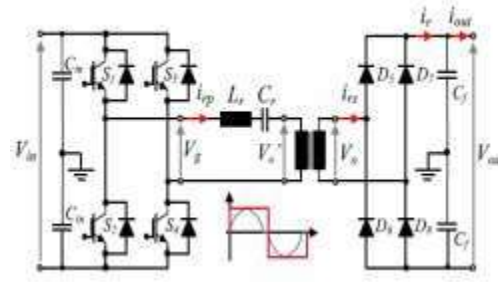
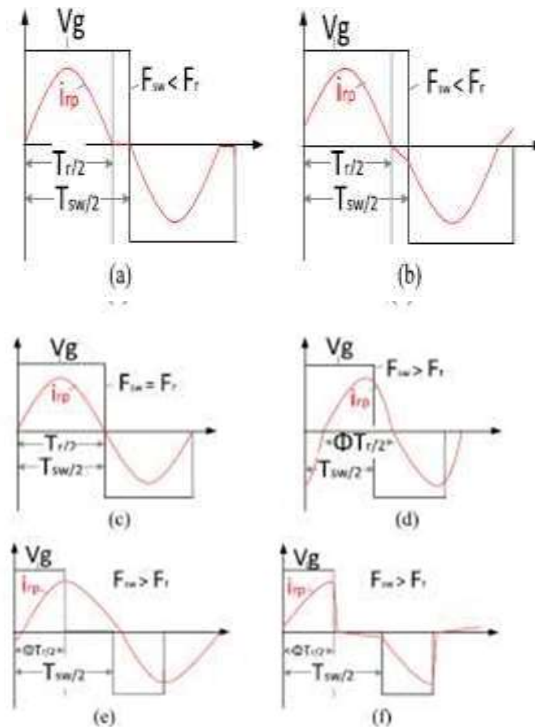


Fig. 3. Series resonant converter.

Possible Modes of Operation

A SRC can operate in three modes: subresonant [see Fig. 4(a) and (b)], resonant [see Fig. 4(c)], and super-resonant [see Fig. 4(d)]. F_{sw} is less than F_r in subresonant mode, but greater in super-resonant mode. In resonant mode, F_{sw} equals that of the resonant tank, implying that switching occurs exactly at the current's zero crossing occurrence. Conductions can exist in two states for both subresonant and super-resonant modes: continuous and discontinuous. The existence of a zero current subinterval characterises DCM [see Fig. 4(a)] for subresonant mode. During this time, all rectifier diodes are reverse biased until V_g changes sign. When the resonant current rings continuously for the entire switching period, CCM [see Fig. 4(b)] occurs. Prior art identifies three alternative control approaches for subresonant and super-resonant modes: frequency control [see Fig. 4(a)–(d)], phase shift control [see Fig. 4(e) and (f)], and dual control [see Fig. 4(g) and (h)].



$$F_r = \frac{1}{2\pi \sqrt{L_r C_r}}$$

$$\omega_r = 2\pi F_r$$

$$Z_c = \sqrt{\frac{L_r}{C_r}}$$

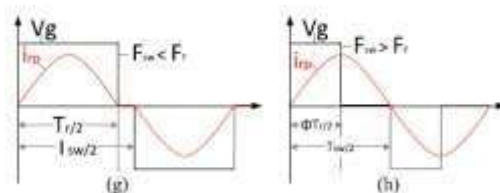


Fig. 4. SRC modes of operation and control methods: frequency control (a)–(d); phase shift control (e) and (f); dual control (g) and (h). (a) Sub-resonant DCM. (b) Sub-resonant CCM. (c) Resonant. (d) Super-resonant CCM. (e) Phase shift superresonant. (f) Phase shift subresonant. (g) Dual control subresonant. (h) Dual control superresonant.

The effective resonant tank impedance varies with the switching frequency due to frequency control of the input voltage. The phase- shift approach regulates the applied voltage to the resonant tank by varying the duty cycle of the inverter (square wave) voltage while keeping the switching frequency constant. It can be used in either super-resonant [see Fig. 4(e)] or sub-resonant [see Fig. 4(f)] mode. Dual control employs a combination of variable frequency and phase shift to manage transformer primary voltage and switching current. Dual control in super-resonant mode [see Fig. 4(h)] has been reported in prior art, however dual control in sub-resonant mode [see Fig. 4(g)] has not been studied.

Selection of Mode of Operation and Control Method

includes a significant big N-base region that stores a substantial quantity of charge during the semiconductor's conduction phase. When the switch is turned off, the stored charge is evacuated from the semiconductor, resulting in tail currents that overlap with the blocking voltage and substantial switching losses. As a result, a mode of operation that allows for zero current switching (ZCS) or a low current upon turn-off must be used. Subresonant mode is hence the obvious mode of operation for IGBT applications.

SIMULATION RESULTS

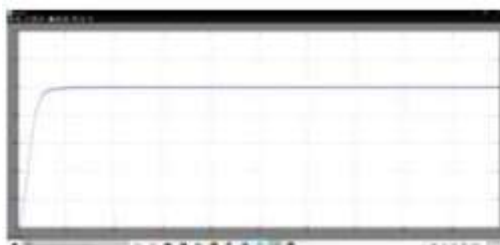
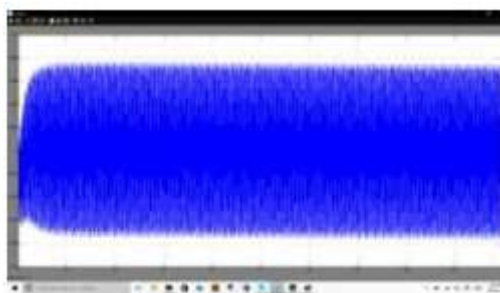


Fig- power



In general, the mode of operation and control method for the SRC are determined by the application type. For example, super resonant and phase shift control are preferred in low power and high voltage applications. A three-phase form of the SRC in resonant mode is described, which offers efficiency more than 99 percent but lacks controllability. Constant frequency and subresonant modes, on the other hand, are used in traction and solid state applications. The mode of operation and control method are determined by the inverter side device and the application requirements. Because of the high power and MV use, 6.5-kV insulated gate bipolar transistors (IGBTs) will be used on the inverter side, while 6.5-kV line frequency diodes will be used on the rectifier side. The majority of the publications that use a resonant topology address low power and LV

applications and employ MOSFETs with switching frequencies in the hundreds of kilohertz range. Superresonant mode is appealing for these applications because it enables for zero voltage switching (ZVS) upon turnon. However, as previously noted, the turn-off losses are the primary contributors to overall losses in IGBT applications. According to the major reason, these semiconductors are characterised by a bipolar power stage that, in order to prevent HV,

Fig- magnetizing current i_m



Fig- primary resonant current i_p

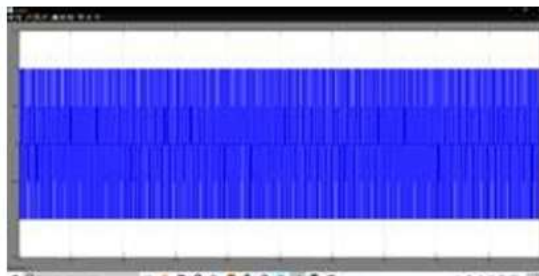


Fig- inverter voltage V_g

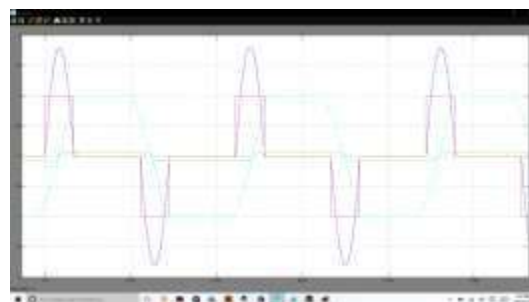


Fig- resonant capacitor voltage V_{cr}



Fig- output current

Fig:5- Simulation results of steady-state operation in DCM1 with steps in switching frequency.

To illustrate the steady-state operation of the target converter, a MATLAB/SIMULINK simulation model was built and run at different switching frequencies, in the range 0–1000 Hz, facilitating the operation in DCM1. The results are shown in Fig. 5 and point out that output power is related to the applied switching frequency. As the converter operates in DCM1, peak resonant current and voltage are constant in the whole operating range.



Fig:6- Simulation results of zoomed in windows of principle waveforms (primary resonant current i_{Rp} , magnetizing current i_m , inverter voltage V_g , and resonant capacitor voltage V_{cr} at 900 Hz. Fig:7- Simulation results of zoomed in windows of principle waveforms (primary resonant current i_{Rp} , magnetizing current i_m , inverter voltage V_g , and resonant capacitor voltage V_{cr} at 450 Hz.

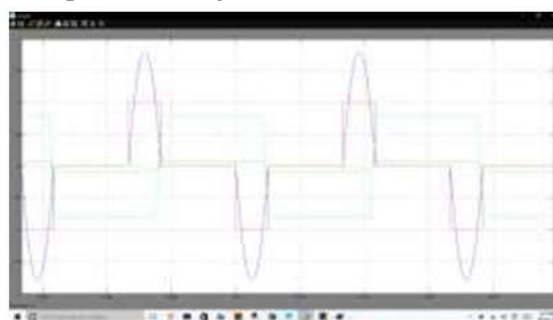


Fig:8- Simulation results of zoomed in windows of principle waveforms (primary resonant current i_{Rp} , magnetizing current i_m , inverter voltage V_g , and resonant capacitor voltage V_{cr} at 150 Hz.

Fig. 6, 7, 8 are zoomed in windows of the principle current and voltage waveforms (primary current i_{Rp} , secondary current i_{Rs} , inverter voltage V_g , capacitor voltage V_{Cr} , magnetizing current i_m) and they also demonstrate how pulse removal technique impacts the magnetizing current, keeping it constant, regardless of applied frequency.

CONCLUSION

Due to its great efficiency and small transformer size, the SRC with resonant tank on the HV side is presented as a possibility for megawatt HV dc wind turbines. For high-power resonant topologies, frequency management in subresonant is recognised as an optimal control strategy for controlling output power and increasing efficiency. The disadvantage is that the transformer must be designed for the lowest working



point. To address this issue, a new way of operation known as pulse removal is introduced. In subresonant mode, variable frequency and phase shift are utilised to control output power, and the basic objective is to clamp the applied voltage to zero as soon as the resonant current becomes zero, reducing flux build-up on the transformer core. The paper focuses on the analysis of SRC# and explores the conduction modes that the topology may encounter when the output voltage lowers. The resonant current and voltage formulae for each mode were presented, together with forecasts of output power, peak voltage, and current stress. The results of a MATLAB/SIMULINK simulation were used to analyse the pulse removal approach and the expected conduction patterns.

REFERENCES

1. C. Meyer, -Key components for future offshore DC grids, Ph.D. dissertation, Inst. Power Elect. Drives, RWTH Aachen University, Aachen, Germany, 2007.
2. C. Meyer and RikW. De Doncker, -Design of three phase series resonant converter for offshore DC grids, in Proc. IEEE Ind. Appl. Annu. Meeting, 2007, pp. 216–223.
3. L. Max, -Design and control of a DC grid for offshore wind farms, Ph.D. dissertation, Dept. Energy Environ, Chalmers University of Tech., Gothenburg, Sweden, 2009.
4. W. Chen, A. Q. Huan, C. Li, G. Wang, and W. Gu, -Analysis and comparison of medium voltage high power DC/DC converters for offshore wind energy systems, IEEE Trans. Power Electron., vol. 28, no. 4, pp. 2014–2023, Apr. 2013.
5. D. Duji, F. Kieferndorf, and F. Canales, -Power electronic transformer technology for traction applications—An overview, in Proc. 7th. Int. Pow. Electron. Motion Contr., 2012, vol. 16, no. 1, pp. 50–56.
6. M. Steiner and H. Reinold, -Medium frequency topology in railway applications, in Proc. Eur. Conf. Power Electron. Appl., 2007, pp. 1–10.
7. H. Hoffmann and B. Piepenbreier, -Medium frequency transformer in resonant switching dc/dc-converters for railway applications, in Proc. 14th Eur. Conf. Power Electron. Appl., 2011, pp. 1–8.
8. L. Heinemann, -An actively cooled high power, high frequency transformer with high insulation capability, in Proc. 17th Annu. IEEE Appl. Power Electron. Conf. Expo., 2002, vol. 1, pp. 352–357.
9. J. W. Kolar and G. I. Ortiz, -Solid state transformer concepts in traction and smart grid applications schedule/outline, in Proc. Int. Power Electron. Motion Control Conf., 2012, pp. 1–166.
10. G. I. Ortiz, -High-power DC-DC converter technologies for smart grid and traction applications, Ph.D. dissertation, Inst. Power Elect. Drives, ETH Zurich, Zurich, Switzerland, 2014.
11. J. E. Huber and J.W. Kolar, -Analysis and design of fixed voltage transfer ratio DC/DC converter cells for phase-modular solid-state transformers, in Proc. IEEE Energy Convers. Congr. Expo., 2015, pp. 5021–5029.